ELSEVIER

www.elsevier.nl/locate/carres

Carbohydrate Research 317 (1999) 131–144

CARBOHYDRATE RESEARCH

Endoglucanase V and a phosphatase from *Trichoderma viride* are able to act on modified exopolysaccharide from *Lactococcus lactis* subsp. *cremoris* B40

Willemiek H.M. van Casteren [a], Mirjam A. Kabel [a], Cor Dijkema [b], Henk A. Schols [a], Gerrit Beldman [a], Alphons G.J. Voragen [a,*]

[a] *Wageningen Agricultural University, Department of Food Technology and Nutritional Sciences, Food Science Group, Bomenweg 2, NL-6703 HD Wageningen, The Netherlands*

[b] *Wageningen Agricultural University, Department of Biomolecular Sciences, Laboratory of Molecular Physics, Dreijenlaan 3, NL-6703 HA Wageningen, The Netherlands*

Received 17 November 1998; accepted 15 March 1999

Abstract

EPS B40 from *Lactococcus lactis* subsp. *cremoris* consists of a repeating unit of →4)-β-D-Glc*p*-(1→4)-[α-L-Rha*p*-(1→2)][α-D-Gal*p*-1-PO_4-3]-β-D-Gal*p*-(1→4)-β-D-Glc*p*-(1→. A phosphatase from *Trichoderma viride* was able to release phosphate, but only after removal of rhamnosyl and galactosyl residues by mild CF_3CO_2H treatment. Purified endoV from *T. viride* was able to act on the backbone of the polymer, but only if rhamnosyl substituents and phosphate had been removed. After complete removal of phosphate and partial removal of rhamnosyl residues by HF treatment, incubation with endoV resulted in a homologous series of oligomers. Purification of these oligomers and subsequent characterisation by NMR demonstrated that endoV was able to cleave the β-(1→4) linkage between two glucopyranosyl residues when the galactopyranosyl residue towards the nonreducing end is unsubstituted. The mode of action of endoV on HF-treated EPS B40 is discussed on the basis of the subsite model described for endoV [J.-P. Vincken, G. Beldman, A.G.J. Voragen, *Carbohydr. Res.*, 298 (1997) 299–310].

Keywords: Exopolysaccharide; *Lactococcus lactis* subsp. *cremoris*; *Trichoderma viride*; Phosphatase; Endoglucanase; Mode of action

1. Introduction

Some types of endocellulases (EC 3.2.1.4) are able to cleave (1→4)-β-glycosidic linkages in a variety of substrates such as cellulose, carboxymethylcellulose, (1→3), (1→4)-glucan [1,2], xylan [3,4], xyloglucan [5], mannan [6], and a deacetylated heteroglycan produced by *Pseudomonas flavescens* [7]. The cellulase complex of *Trichoderma viride* contains six endoglucanases [8]. Based on their ability to degrade xylans, some of these endoglucanases (endoIV, V and VI) have a broader substrate specificity than others (endoI, II and III) [3]. The differences in specificity of glycosyl hydrolases can be defined precisely by the use of substrates with known, and preferably regular, structures [1]. Since microbial heteropolysaccharides are almost all composed of repeating units [9], their regular structures could be very

* Corresponding author. Tel.: +31-317-482-888; fax: +31-317-484-893.

E-mail address: office@chem.fdsci.wau.nl (A.G.J. Voragen)

0008-6215/99/$ - see front matter
PII: S0008-6215(99)00072-5

useful for the characterisation of glycosyl hydrolases.

To study the relationship between the chemical structure and the physical properties of exopolysaccharide (EPS) B40, crude enzyme preparations from the major enzyme manufacturers were screened for activity towards this EPS. It was shown that a cellulase preparation from *T. viride* was able to degrade HF-modified EPS B40 [10]. HF-treated EPS B40 consists of repeating units: probably →4)-β-D-Glc*p*-(1→4)[α - L - Rha*p* - (1→2)] - β - D - Gal*p* - (1→4)-β-D-Glc*p*-(1→, in which part of the rhamnosyl substituents (ca. 20%) have been removed by the HF treatment [10]. Although the endo-activity found was not helpful for studying the structure–function relationship of EPS, the regular structure of this EPS could be very useful for the characterisation of the enzyme. Therefore, the present study investigates the endoglucanase in the cellulase preparation that is responsible for the degradation of HF-treated EPS B40. The influence of side-groups in the substrate on the hydrolysing capability of the enzyme was analysed by incubating the enzyme with chemically modified EPS B40. In addition, the homologous series of oligomeric end products derived from HF-treated EPS B40 was purified and characterised to examine the mode of action of the endoglucanase.

2. Experimental

EPS B40.—Crude EPS produced by *Lactococcus lactis* subsp. *cremoris* B40 [11] was kindly supplied by NIZO Food Research (Ede, The Netherlands). Further purification of EPS B40 was performed using CCl_3CO_2H and EtOH as described by van Casteren et al. [10].

HF-treated EPS B40.—EPS B40 was chemically modified by treatment with 28 M hydrofluoric acid (48 h, 0 °C). During this treatment, terminally linked galactose and phosphate are removed and as a side effect ca. 20% of the rhamnosyl substituents are also removed [10].

CF_3CO_2H-treated (and HF-treated) EPS B40.—(HF-treated) EPS B40 (3 mg) was partially hydrolysed in 2.5 mL 0.1 M CF_3CO_2H (1 h, 100 °C) to remove rhamnosyl substituents. CF_3CO_2H was then removed by repeated evaporation followed by freeze drying.

H_2SO_4-treated EPS B40.—Purified EPS B40 was treated with 0.3 M H_2SO_4 (2 h, 37 °C) as described by van Casteren et al. [10] to remove terminally linked galactose.

Enzymes.—Maxazyme Cl from *T. viride* (Gist-brocades, Delft, The Netherlands) and endoglucanase V (endoV, EC 3.2.1.4) purified from this preparation by Beldman et al. [8] were used. Since the nomenclature of our endoglucanases differs from the one generally adopted in literature, endoV has been tentatively identified as being EGI [4,12].

Degradation of modified EPS B40 by Maxazyme Cl.—HF-treated EPS B40, HF- *and* CF_3CO_2H-treated EPS B40 and CF_3CO_2H-treated EPS B40 were incubated with Maxazyme Cl as described in Ref. [10]. The resulting degradation products were analysed by HPAEC and MALDI-TOF MS. To obtain sufficient oligomeric fragments for purification and subsequent characterisation by NMR, HF-modified EPS B40 (0.3 g) was dissolved in 150 mL 50 mM NaOAc buffer (pH 5). Maxazyme Cl (0.33 g) was dissolved and dialysed against the same buffer (final volume: 23 mL). The substrate (140 mL) was incubated (24 h, 30 °C) with dialysed enzyme solution (20 mL). The protein content was ca. 0.01% according to the procedure of Bradford [13] using BSA as standard. After incubation, the enzymes were denatured by heating (15 min, 100 °C). Finally, the sample was centrifuged and the supernatant was freeze dried and used for isolation of the oligosaccharides.

Incubation of HF-treated EPS B40 with endoV.—HF-treated EPS B40 in 50 mM NaOAc, pH 5.0 (0.25 mL, 2 mg/mL) was incubated (24 h, 30 °C) with purified endoV (ca. 0.5 μg protein). The sample was then heated (15 min, 100 °C), centrifuged and analysed by HPAEC and MALDI-TOF MS.

Incubation of CF_3CO_2H-treated (and HF-treated) EPS B40 with endoV.—CF_3CO_2H-treated samples (3 mg) were dissolved in 1 mL 50 mM NaOAc pH 5.0. Part of this solution (0.1 mL) was incubated (24 h, 30 °C) with purified endoV (ca. 0.2 μg protein). Then, the samples were heated (15 min, 100 °C), cen-

trifuged and analysed by HPAEC and MALDI-TOF MS.

Release of oligosaccharides from HF-treated EPS B40 in time.—Purified endoV (ca. 0.2 μg) was added to HF-treated EPS B40 in 50 mM NaOAc pH 5.0 (1.7 mL, 2.2 mg/mL). During incubation at 20 °C, a sample was taken each hour for analysis by HPAEC. The amount of an oligomer released in a certain time interval was expressed as a percentage of the PAD response of this oligomer peak after incubation for 20.5 h.

Size-exclusion chromatography.—The oligomers obtained after preparative degradation of HF-treated EPS B40 with Maxazyme Cl were purified using columns (100 × 2.6 cm, i.d.) of BioGel P-6 and BioGel P-2 (BioRad). After the sample (at most 120 mg per run) had been applied onto the column, elution with distilled water (0.5 mL/min) was performed at 60 °C. The refractive index was monitored on-line (Shodex RI-72 detector) and appropriate fractions were pooled. The purity of the pools was checked using HPAEC and if necessary pools were rechromatographed.

HPAEC analysis of the digests.—Degradation products were analysed on a CarboPac PA-1 column using HPAEC equipment as described earlier [10]. After equilibration with 16 mM NaOH, 20 μL sample was injected and the elution program was started: 0 → 20 min, 16 mM NaOH isocratic; 20 → 25 min, 0.1 M NaOH isocratic; 25 → 65 min, linear gradient of 0 → 0.4 M NaOAc in 0.1 M NaOH; 65 → 70 min, 1 M NaOAc in 0.1 M NaOH isocratic; followed by a conversion step to NaOH (70 → 75 min, 0.1 M NaOH isocratic) and re-equilibration (75 → 90 min, 16 mM NaOH isocratic).

HPSEC analysis of CF_3CO_2H-treated polymers.—HPSEC was performed as has been described by van Casteren et al. [10], although this time a Spectra System P1000 pump and an AS 3000 autosampler were used.

MALDI-TOF MS analysis of the digest.—The digest of modified EPS B40 (10 μL) was desalted with Dowex (AG 50W-X8 Resin; BioRad 143-5441) and then mixed on plate (1 μL) with 1 μL matrix. The matrix was made by mixing isocarbostyril (3 mg), 2,5-dihydroxybenzoic acid (9 mg), acetonitrile (0.3 mL) and distilled water (0.7 mL). Matrix-assisted laser desorption ionisation time of flight mass spectrometry (MALDI-TOF MS) was performed using a Voyager-DE RP Biospectrometry Workstation (PerSeptive Biosystems, Framingham, USA) in the positive mode. The negative mode was used as well to examine whether phosphate-containing oligosaccharides were released. The laser intensity was set at 2000 which equals 7.5 μJ per pulse. The pulse delay time was 200 ns, the accelerating voltage was 12,000 V, the grid voltage was 7200 V and the guide wire voltage was 9.6 V. The instrument was used in the reflector mode. The mass spectrometer was calibrated using a mixture of galacturonic acid oligomers. Each run, the calibration was checked by analysing a sample of glucosyl oligomers.

Phosphate analysis.—The relative amounts of bound and free phosphate in the samples were determined by comparing the samples with and without destruction in 72% $HClO_4$ (20 min, 180 °C). After dilution, the samples were analysed as described by Chen et al. [14].

Absolute configurations of monosaccharides.—The absolute configurations of the monosaccharides were determined as described by Gerwig et al. [15]. The GC-FID analysis of the trimethylsilated (−)-2-butyl glycosides was performed in a Carlo Erba HRGC 5160 gas chromatograph, equipped with a CP-Sil 5 CB column (25 m × 0.32 mm, Chrompack). The temperature program was: 135 → 160 °C at 0.5 °C/min; 160 → 200 °C at 10 °C/min. The injection-port and detector temperatures were 200 and 250 °C, respectively. The He flow-rate was 3 mL/min and the samples (ca. 0.05 μL) were injected directly on the column without stream splitter.

NMR spectroscopy.—Prior to NMR analysis, the samples were exchanged three times in D_2O (99.9 atom% D, Cambridge Isotope Laboratories, USA) with intermediate freeze drying. Finally, samples were dissolved in 99.96% D_2O (Cambridge Isotope Laboratories, USA). NMR spectra were recorded at probe temperatures of 27 °C (oligosaccharides) or 70 °C

(polysaccharide) on a Bruker AMX-500 spectrometer located at the Wageningen NMR Centre. Chemical shifts are expressed in ppm relative to internal acetone: δ 2.225 for ^{1}H and δ 31.077 for ^{13}C. For small sample amounts Shigemi tubes (Campro Scientific, Veenendaal, The Netherlands) with a sample volume of 190 μL were used.

In 1D ^{1}H NMR spectra, suppression of the HOD signal was achieved by using presaturation during relaxation delay for 1 s. Proton-decoupled ^{13}C spectra were recorded at 125.770 MHz. For 1D ^{1}H and ^{13}C NMR spectra, data sets of 16,384 and 32,768 data points were recorded, respectively.

2D COSY spectra were acquired in the magnitude mode. 2D TOCSY and ROESY spectra were basically acquired as described by Fransen et al. [16] using the time-proportional phase increment (TPPI) method [17]. For 2D HMBC spectra [18] a standard gradient-enhanced 2D-heteronuclear proton detected multiple-quantum coherence pulse-sequence (HMQC) delivered by Bruker was changed into an HMBC sequence by setting the delay between the first proton and first carbon pulse to 60 ms. For all homonuclear 2D experiments, 512 experiments of 2048 data points were acquired with 32–320 scans per increment; the 2D HMBC spectra were acquired in 1024 experiments of 2048 data points.

Time-domain data were multiplied by phase-shifted (squared-)sine-bell functions or with Lorentzian-to-Gaussian multiplication. After zerofilling and Fourier transformation, data sets of 2048 × 1024 or 2048 × 2048 points were obtained which were baseline corrected when necessary.

3. Results

Degradation of modified EPS B40 by Maxazyme Cl.—HF-treated EPS B40 was incubated with Maxazyme Cl, and the digest was analysed by HPAEC. Fig. 1 shows that enzymic digestion resulted in a series of oligomers eluting between 35 and 60 min. The peaks at 12, 14 and 27 min originated from the enzyme preparation. Using on-line HPAEC/MS [19] masses could be assigned to the HPAEC peaks. However, since the HPAEC/MS set-up was not always available, masses of the released oligomers throughout the research were monitored using MALDI-TOF MS. Fig. 2 shows the MALDI-TOF mass spectrum of HF-treated EPS B40 after incubation with Maxazyme Cl. A homologous series of sodiated oligomers was detected, corresponding to the results of HPAEC/MS. Therefore, the masses in Fig. 2 could be assigned to the oligomer peaks in Fig. 1: **1** = 527.1 g/mol, **2** = 1159.4 g/mol, **3** = 1791.6 g/mol, etc. Since MS shows masses of sodiated oligomers, the mass of oligomer **1** corresponds to a trimer of hexoses. Oligomer **2** represents a heptamer of six hexoses and one deoxyhexose. Oligomer **3** is an undecamer of nine hexoses and two deoxyhexoses, etc. Thus, it could be concluded that the enzyme preparation was able to release a series of oligomers starting

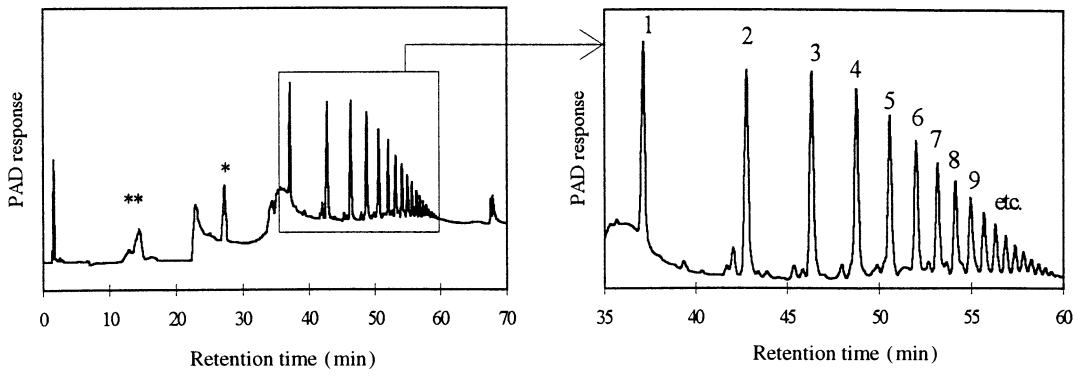

Fig. 1. HPAEC elution profile of a digest of HF-treated EPS B40 after incubation with Maxazyme Cl. *, peaks that originate from the enzyme preparation. The numbering of the oligomer peaks in the enlarged part of the chromatogram indicates the amount of 'repeating units' within the backbone of the oligomer concerned and this numbering is used throughout the paper.

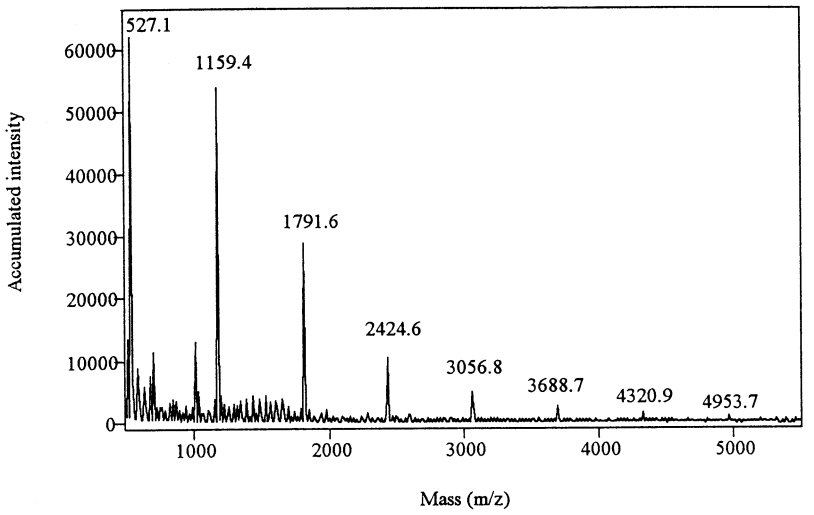

Fig. 2. MALDI-TOF mass spectrum of the digest of HF-treated EPS B40 after incubation with Maxazyme Cl. The masses could be assigned to the HPAEC peaks in Fig. 1: 527.1 = trimer = **1**, 1159.4 = heptamer = **2**, 1791.6 = undecamer = **3**, etc.

with a trimer with an increment of 632 g/mol: three hexoses + [three hexoses + one deoxyhexose]$_n$. Considering the sugar composition of HF-treated EPS B40 [10], the hexoses must be glucose and galactose and the deoxyhexose rhamnose.

HF-treated EPS B40 consists of repeating units: →4)-β-D-Glc*p*-(1→4)[α-L-Rha*p*-(1→2)]-β-D-Gal*p*-(1→4)-β-D-Glc*p*-(1→ (vide infra), in which part of the rhamnosyl substituents (ca. 20%) have been removed during the HF treatment [10]. The absolute configuration of the sugar residues was confirmed. Since all oligomers released during enzyme incubation contained one 'repeating unit' without rhamnosyl substitution, apparently the enzyme is only able to cleave the polymer if rhamnosyl residues have been removed. To confirm this, HF-treated EPS B40 was partially hydrolysed using CF_3CO_2H to remove more rhamnosyl residues. It was calculated from the amount of rhamnose released (HPAEC, not shown) that after this treatment ca. 60% of the repeating units were free of rhamnosyl substitution. Although HPSEC analysis after treatment with CF_3CO_2H showed partial depolymerisation of the EPS, no significant amounts of oligomers were released during this acidic treatment (HPAEC). Incubation of HF- *and* CF_3CO_2H-treated EPS B40 with Maxazyme Cl and analysis by HPAEC showed that there was an increase of oligomer **1** (×6) and oligomer **2** (×2), a decrease of oligomers **3** and **4** and disappearance of oligomer **5** and larger oligomers in comparison with the products of enzyme incubation with HF-treated EPS B40. These results show that indeed the enzyme is able to release smaller oligomers when more rhamnosyl substituents have been removed.

Maxazyme Cl appeared not to be active on EPS B40 [10], which consists of a repeating unit (vide infra): →4)-β-D-Glc*p*-(1→4)[α-L-Rha*p*-(1→2)][α-D-Gal*p*-1-PO_4-3]-β-D-Gal*p*-(1→4)-β-D-Glc*p*-(1→. One of the reasons for this is the presence of rhamnosyl substituents. However, it is possible that the galactose 1-phosphate side groups also obstruct enzyme action. To examine whether this is the case, EPS B40 was partially hydrolysed using CF_3CO_2H. During this treatment, not only ca. 60% of rhamnosyl residues are removed but also the galactosyl residues terminally linked to phosphate, since galactose 1-phosphate is sensitive towards dilute acid [10,20]. Incubation of CF_3CO_2H-treated EPS B40 with Maxazyme Cl did not result in a significant release of phosphate-containing oligomers as was determined by using HPAEC and MALDI-TOF MS. Surprisingly, oligomer **1** (trimer) was released, whereas oligomers **2**, **3**, **4**, etc. were not detected (data not shown). The release of oligomers free of phosphate was unexpected and indicates that either the galactose 3-phosphate linkage was hydrolysed upon CF_3CO_2H treatment or the crude enzyme preparation

contains a phosphatase that is able to cleave this linkage. This was investigated further using the purified enzyme and is discussed below.

Degradation of modified EPS B40 by endoV.—Incubation of HF-treated EPS B40 with endoV purified from Maxazyme Cl released the same oligomers, identified by HPAEC and MALDI-TOF MS, as Maxazyme Cl, indicating that only one enzyme was involved in this degradation. Incubation of HF- *and* CF_3CO_2H-treated EPS B40 with endoV also showed the same degradation pattern, identified by HPAEC and MALDI-TOF MS, as Maxazyme Cl. Since all oligomers released during enzyme incubation contained one 'repeating unit' without rhamnosyl substitution, it was confirmed that endoV is blocked by rhamnosyl residues in EPS B40.

To examine whether endoV is additionally blocked by the phosphate groups on EPS B40, CF_3CO_2H-treated EPS B40 was incubated with endoV. The resulting HPAEC pattern showed no oligomer peaks and the MALDI-TOF mass spectrum did not show a series of 'neutral' oligomers or phosphate-containing peaks. These results indicate that indeed endoV is blocked by phosphate on EPS B40. The fact that endoV did not release oligomer **1** from CF_3CO_2H-treated EPS B40 while Maxazyme Cl did, suggests that the galactose 3-phosphate linkage was not hydrolysed during the CF_3CO_2H treatment. It is likely then, that Maxazyme Cl contains a phosphatase able to cleave this linkage. Since rhamnosyl residues had already been removed during the CF_3CO_2H treatment, the release of phosphate by such an enzyme would make the substrate accessible to endoV, explaining the release of oligomer **1**.

Degradation of modified EPS B40 by a phosphatase.—The indication for the presence of a phosphatase in Maxazyme Cl was supported by the amount of free phosphate in the digests, expressed as a percentage of the total phosphate content: during incubation of CF_3CO_2H-treated EPS B40 with Maxazyme Cl the amount of free phosphate increased from $< 10\%$ to ca. 60%. Maxazyme Cl itself did not contribute to the total amount of phosphate. The fact that there was almost no free phosphate in native EPS B40 after treatment with Maxazyme Cl suggests that the phosphatase only acts if terminally linked galactose and/or rhamnose is absent from the EPS. Treatment of EPS B40 with dilute H_2SO_4 (37 °C) results in a release of galactose, since the galactose 1-phosphate linkage is sensitive towards dilute acid [10]. During this treatment, the rhamnosyl linkages were not hydrolysed. Incubation of H_2SO_4-treated EPS B40 with Maxazyme Cl did not result in a release of phosphate, indicating that the phosphatase in Maxazyme Cl is hindered by rhamnosyl residues in EPS B40. Since we were not able to modify EPS B40 to generate a substrate without rhamnosyl residues but still carrying terminally linked galactose moieties, we were not able to check whether the phosphatase is also hindered by the presence of terminally linked galactose.

Release of oligosaccharides from HF-treated EPS B40 in time.—Fig. 3 shows the time course of the release of oligomers **1**, **7** and **11** from HF-treated EPS B40 during incubation with endoV. The oligomers shown are representative of the trend for other oligomers released: the larger the oligomers the faster they accumulate. For oligomers larger than **11**, the

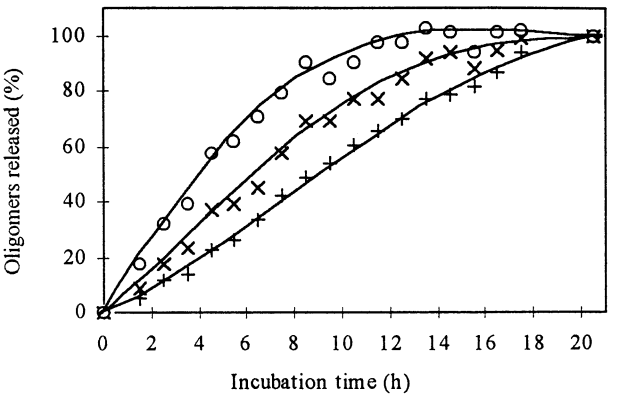

Fig. 3. Release of oligomers **1**, **7** and **11** (DP 3, 27, 43) from HF-treated EPS B40 in time during incubation with endoV. The amounts of released oligomers are expressed as a percentage of the PAD response of this oligomer peak after incubation for 20.5 h. +, oligomer **1** (Fig. 1); ×, oligomer **7** (Fig. 1); ○, oligomer **11** (Fig. 1). It should be noted that the decreasing resolution of the HPAEC system with increasing size of oligomers influenced the results (see text).

Table 1
^{1}H NMR chemical shifts[a] of the trimer **1** isolated from HF-modified EPS B40 after treatment with Maxazyme Cl as determined from COSY, TOCSY and ROESY

Residue **1**	H-1	H-2	H-3	H-4	H-5	H-6a	H-6b
A	4.67	3.34	3.50	3.40	3.43	3.91	3.73
B	4.48	3.61	3.77	4.18	3.80	[b]	[b]
C$^{\alpha}$	5.22	3.57	3.83	3.65	3.95	[c]	[c]
C$^{\beta}$	4.66	3.28	3.63	3.66	3.59	3.95	3.80

[a] In ppm relative to the signal of acetone at δ 2.225.
[b] Between δ 3.85 and 3.70.
[c] Between δ 3.96 and 3.82.

amount released after 12–18 h was higher than after 20 h. This indicates that large oligomers were not only released but also further degraded during incubation. Due to a decreasing resolution of the HPAEC analysis with increasing size of oligomers, there is no discrimination between end products in which one 'repeating unit' is free of rhamnosyl residues and intermediate products with, for example, two 'repeating units' free of rhamnosyl residues. Thus, the results in Fig. 3 can be explained by the fact that before reaching the end point of the incubation, the HPAEC peaks of large oligomers contain both intermediate products and end products.

As stated above, incubation of HF-treated EPS B40 with endoV resulted in a series of oligomers starting with a trimer: three hexoses + [three hexoses + one deoxyhexose]$_n$. Since the exact structure of these oligomers is still unknown, no information is provided on the precise mode of action of endoV towards this substrate. To enable identification of the oligomers, the substrate was treated with the enzyme on a larger scale and the oligomers obtained purified and analysed by NMR. Since the availability of pure endoV was limited and since incubation with Maxazyme Cl resulted in the same series of oligomers, Maxazyme Cl was used for the preparative incubation. The oligomers were purified using size exclusion chromatography and the effectiveness confirmed by HPAEC.

NMR spectroscopy of trimer **1**.—The 1D ^{1}H NMR spectrum of the trimer **1** showed four resonances in the anomeric region, which were designated **A** H-1–**C**$^{\alpha/\beta}$ H-1 (Fig. 4(a)). The coupling constant of the narrow doublet at δ 5.22 (**C**$^{\alpha}$ H-1, $^3J_{1,2}$ 3.8 Hz) suggests the presence of an α-hexopyranosyl residue. The coupling constants of the broader doublets at δ 4.67 (**A** H-1, $^3J_{1,2}$ 8.1 Hz), 4.66 (**C**$^{\beta}$ H-1, $^3J_{1,2}$ 8.1 Hz) and 4.48 (**B** H-1, $^3J_{1,2}$ 7.8 Hz) indicate the presence of β-hexopyranosyl residues. The intensity ratio of **A** H-1: **B** H-1: **C**$^{\alpha}$ H-1: **C**$^{\beta}$ H-1 was 1:1:0.3:0.7. Therefore, the resonances at δ 5.22 and 4.66 were assigned to the sugar residue at the reducing end (residue **C**) since both anomers exist because of mutarotation.

The 2D COSY, TOCSY and ROESY measurements (not shown) allowed the assignment of the protons as given in Table 1. The resonances of **A** H-1 and **C**$^{\beta}$ H-1 had correlations to H-2, 3, 4, 5, 6a, 6b in the TOCSY spectrum, identifying glucose residues. The resonance of **B** H-1 only showed TOCSY cross-peaks to H-2, 3, 4; due to inefficient magnetisation transfer through the small $^3J_{3,4}$ and $^3J_{4,5}$ couplings no correlations to H-5 could be seen [16,21]. This, combined with the characteristic resonance position of H-4, allowed the assignment of residue **B** as a galactosyl residue.

Methylation analysis of HF-treated EPS B40 demonstrated the presence of 1,4-linked glucosyl residues, 1,2,4-linked galactosyl residues and terminally linked rhamnosyl residues [10]. For the trimer, the differences in the chemical shifts (Table 1) of residue **A** H-4 ($\Delta\delta$ −0.005), **B** H-4 ($\Delta\delta$ 0.235), **C**$^{\alpha}$ H-4 ($\Delta\delta$ 0.255) and **C**$^{\beta}$ H-4 ($\Delta\delta$ 0.255) compared with the chemical shifts for the corresponding aldohexoses reported by Bock and Thøgersen [22] indicate that **B** and **C**$^{\alpha/\beta}$ are linked at C-4 but residue **A** is not. The 2D ROESY spectrum showed two intense interresidual cross-peaks

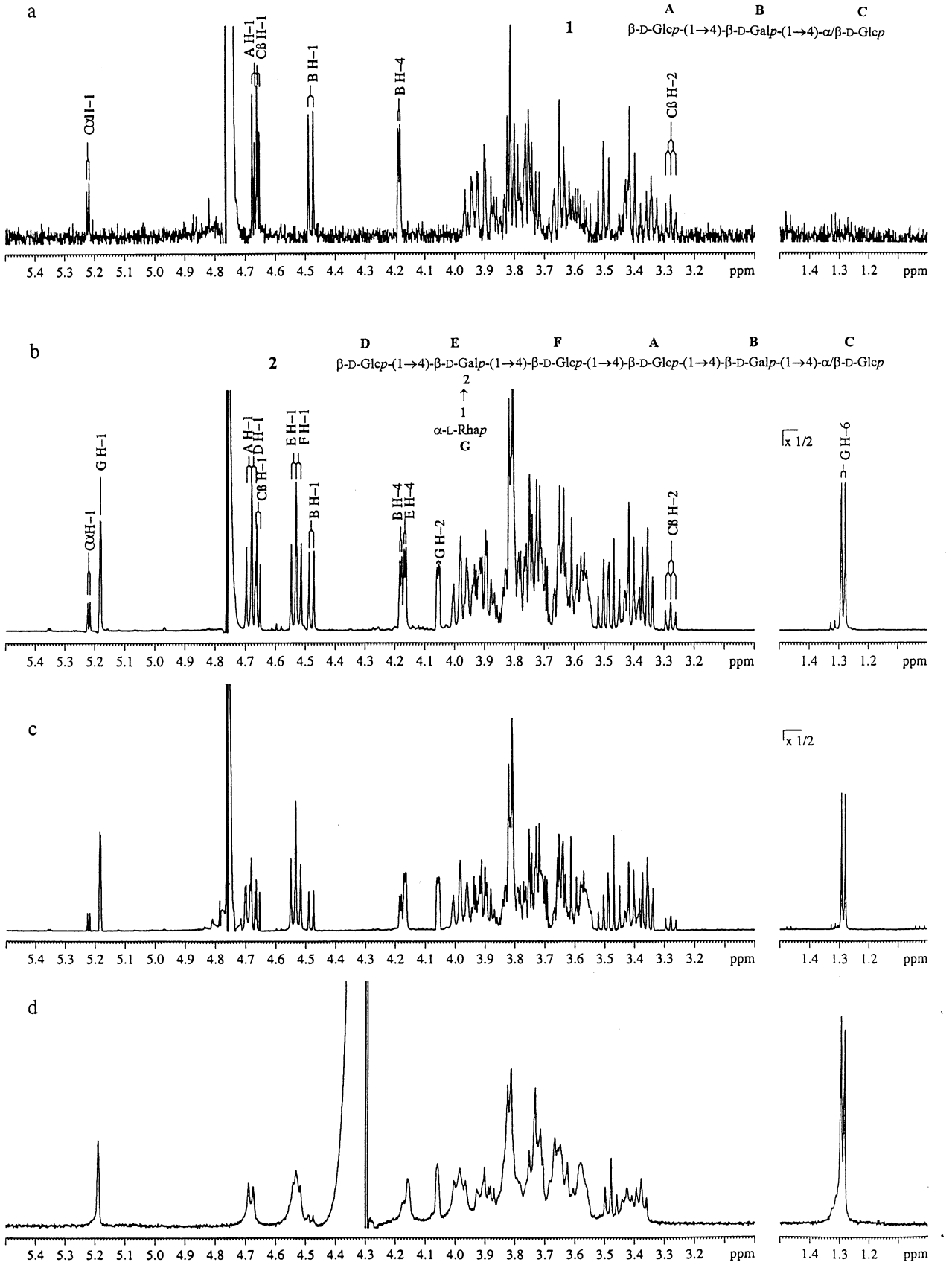

Fig. 4. 500 MHz ^{1}H NMR spectra of (a) trimer **1**, (b) heptamer **2**, (c) undecamer **3** and (d) HF-treated EPS B40, recorded in D_2O at 27 °C (oligosaccharides) or 70 °C (polysaccharide).

(**A** H-1, **B** H-4 and **B** H-1, $\mathbf{C}^{\beta}$ H-4) resulting in structure **1** shown in Fig. 4(a). Unfortunately, the results could not be confirmed with an HMBC experiment due to the low signal-to-noise ratio as a result of the low sample concentration.

Since the incubation of HF-treated EPS B40 with Maxazyme Cl resulted in the release of oligomer **1** (amongst others), endoV must have cleaved the polymer between two glucosyl residues. As shown, endoV is hindered by the presence of rhamnosyl residues in the polymer and all oligomers released contained exactly one repeating unit free of terminally linked rhamnose. These results suggest that endoV releases oligomers containing an unsubstituted 'repeating unit' at the reducing side or the nonreducing side of the glycosidic linkage cleaved. This was investigated further by NMR analysis of the heptamer.

NMR spectroscopy of heptamer **2**.—The 1D ^{1}H NMR spectrum of the heptamer **2** showed the presence of eight resonances in the anomeric region, which were designated **A**–**G** (Fig. 4(b)). The coupling constants of the resonance at δ 5.23 ($\mathbf{C}^{\alpha}$ H-1, $^3J_{1,2}$ 3.8 Hz, $^1J_{\text{C-1,H-1}}$ 169 Hz) suggested the presence of an α-hexopyranosyl residue. The coupling constants of the resonances at δ 4.69 (**A** H-1, $^3J_{1,2}$ 8.7 Hz, $^1J_{\text{C-1,H-1}}$ 166 Hz), 4.67 (**D** H-1, $^3J_{1,2}$ 8.2 Hz, $^1J_{\text{C-1,H-1}}$ 163 Hz), 4.66 ($\mathbf{C}^{\beta}$ H-1, $^3J_{1,2}$ 7.9 Hz, $^1J_{\text{C-1,H-1}}$ 163 Hz), 4.54 (**E** H-1, $^3J_{1,2}$ 8.2 Hz, $^1J_{\text{C-1,H-1}}$ 166 Hz), 4.52 (**F** H-1, $^3J_{1,2}$ 8.4 Hz, $^1J_{\text{C-1,H-1}}$ 166 Hz), and 4.48 (**B** H-1, $^3J_{1,2}$ 7.8 Hz, $^1J_{\text{C-1,H-1}}$ 163 Hz) indicate the presence of β-hexopyranosyl residues. The resonances at δ 5.23 and 4.66 showed an intensity ratio of 0.3:0.7 (the intensities of the other anomeric resonances being 1) and were assigned to the sugar at the reducing end (residue $\mathbf{C}^{\alpha/\beta}$). The rhamnosyl residue **G** (**G** H-1 δ 5.19, $^3J_{1,2}$ 1.4 Hz, $^1J_{\text{C-1,H-1}}$ 175 Hz) showed a high-field doublet at δ 1.28 (**G** H-6, $^3J_{5,6}$ 6.3 Hz) arising from the methyl group.

Using the ^{1}H NMR data, the 2D COSY (not shown) and TOCSY (not shown) measurements a complete assignment of the rhamnosyl (residue **G**) protons, starting from the methyl doublet (Table 2), was possible. The chemical shift of **G** H-5 at δ 3.90 strongly suggests an α configuration for residue **G** [23]. From the 2D COSY, TOCSY and ROESY measurements (not shown), most protons of the other residues (**A**–**F**) could also be assigned (Table 2). The resonances of **B** H-1 and **E** H-1 only showed cross-peaks to H-2, 3, 4 in the TOCSY spectra, whereas the other anomeric protons had correlations to H-2, 3, 4, 5, 6a, 6b. Together with the characteristic resonance positions of **B** H-4 and **E** H-4, residues **B** and **E** were assigned to galactosyl residues. Residues **A**, $\mathbf{C}^{\alpha/\beta}$, **D** and **F** were identified as glucosyl residues. The differences in the chemical shifts (Table 2) of residues **A** H-4 ($\Delta\delta$ 0.245), **B** H-4 ($\Delta\delta$ 0.235), $\mathbf{C}^{\alpha}$ H-4 ($\Delta\delta$ 0.245), $\mathbf{C}^{\beta}$ H-4 ($\Delta\delta$ 0.255), **D** H-4 ($\Delta\delta$ −0.005), **E** H-4 ($\Delta\delta$ 0.225) and **F** H-4 ($\Delta\delta$ 0.345), compared with the chemical shifts of the corresponding aldohexoses reported by Bock and Thøgersen [22], suggest that all of these residues except for residue **D** are substituted at H-4. As a consequence, **D** was as-

Table 2
^{1}H NMR chemical shifts[a] of the heptamer **2** isolated from HF-modified EPS B40 after treatment with Maxazyme Cl as determined from COSY, TOCSY and ROESY

Residue **2**	H-1	H-2	H-3	H-4	H-5	H-6a	H-6b
A	4.69	3.38	3.65	3.65	3.56	3.97	3.82
B	4.48	3.62	3.78	4.18	3.81	n.d.[b]	n.d.
$\mathbf{C}^{\alpha}$	5.23	3.57	3.83	3.65	3.94	n.d.	n.d.
$\mathbf{C}^{\beta}$	4.66	3.28	3.63	3.66	3.60	3.95	3.80
D	4.67	3.35	3.51	3.40	3.43	3.91	3.74
E	4.54	3.72	3.92	4.17	n.d.	n.d.	n.d.
F	4.52	3.35	3.61	3.75	3.57	4.00	3.79
G	5.19	4.06	3.70	3.47	3.90	1.28	1.28

[a] In ppm relative to the signal of acetone at δ 2.225.
[b] n.d., not determined.

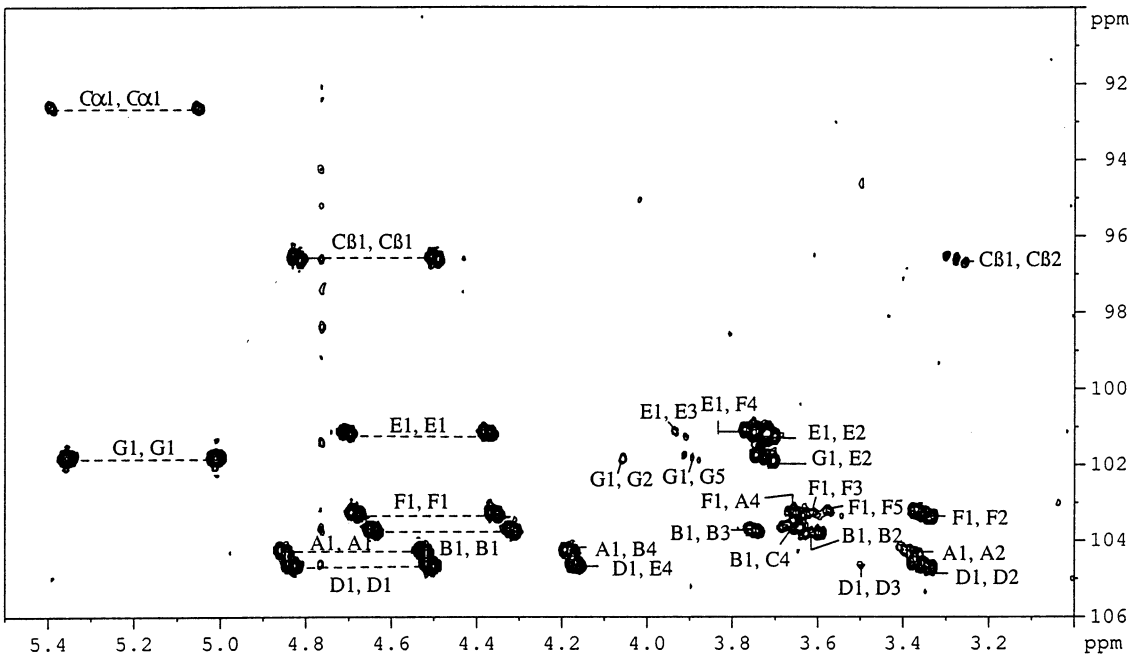

Fig. 5. Partial 500 MHz 2D $^{13}C-^{1}H$ HMBC NMR spectrum of heptamer **2** recorded in D_2O at 27 °C. The code E1, F4 corresponds to the coupling between **E** C-1 and **F** H-4, etc.

signed to the sugar residue at the nonreducing end of the heptamer. The relative large chemical shift of **E** H-2 (δ 3.72) compared with **B** H-2 (δ 3.62) suggests that galactosyl residue **E**, unlike residue **B**, is substituted at O-2.

Comparison of the proton chemical shifts of **1** (Table 1) and **2** (Table 2) shows close similarity for residues designated with the same letter, except for residue **A**. This exception was caused by the fact that **A** is a (1→4)-linked glucosyl residue in **2** while it is a terminally linked glucosyl residue in **1**. The designations used are **A** for a glucosyl residue linked to an unsubstituted galactosyl residue and **D** for a glucosyl residue linked to a substituted galactosyl residue (vide infra). The consequence of this designation is that residues with similar chemical shifts (**A** in **1** and **D** in **2**; both glucosyl residues at the nonreducing end) are designated differently.

The 1D ^{13}C NMR spectrum (not shown) of **2** showed eight anomeric signals. This is in agreement with the heptasaccharide since two resonances were expected for residue **C**. Based on their chemical shifts, the C-1 signals at δ 96.6 and 92.7 were assigned to the glucosyl residue at the reducing end ($\mathbf{C}^{\beta}$ and $\mathbf{C}^{\alpha}$, respectively). The CH_3 signal of the rhamnosyl residue (**G**) was observed at δ 17.3 and the C-6 signals of the other residues were found between δ 62.0 and 60.0. These positions of the C-6 signals are in favour of the absence of 6-linked hexosyl residues and the occurrence of pyranose rings only (comparison of chemical shifts: [22]).

The 2D ROESY spectrum showed intense interresidual cross-peaks between: **G** H-1, **E** H-2; **A** H-1, **B** H-4; **D** H-1, **E** H-4; **B** H-1, $\mathbf{C}^{\alpha/\beta}$ H-4 or **A** H-4; **F** H-1, $\mathbf{C}^{\alpha/\beta}$ H-4 or **A** H-4. The correlation between **E** H-1 and **F** H-4 could only be assigned tentatively, due to overlap in the spectra. The 2D $^{13}C-^{1}H$ HMBC spectrum of **2** (Fig. 5) allowed the complete assignment of the anomeric ^{13}C signals: δ 104.6: **D** C-1; 104.3: **A** C-1; 103.7: **B** C-1; 103.3: **F** C-1; 101.8: **G** C-1; 101.2: **E** C-1; 96.6: $\mathbf{C}^{\beta}$ C-1 and 92.7: $\mathbf{C}^{\alpha}$ C-1. Most other ^{13}C resonances could be assigned as well. Using the assignments of the ^{13}C and ^{1}H signals in the HMBC spectrum, the long-range correlations observed across the glycosidic linkages could be interpreted: **D** C-1, **E** H-4; **E** C-1, **F** H-4; **F** C-1, **A** H-4; **A** C-1, **B** H-4; **B** C-1, $\mathbf{C}^{\alpha/\beta}$ H-4; and **G** C-1, **E** H-2. The possibility of having confused the assignments of **A** H-4 and $\mathbf{C}^{\alpha/\beta}$ H-4 was ruled out since the strong interaction between **A** C-1 and **B** H-4 excludes interaction between **B** C-1 and **A** H-4. The correlations in the

HMBC and ROESY spectra determined the complete monosaccharide sequence of the heptamer **2** resulting in the structure shown in Fig. 4(b).

NMR spectroscopy of undecamer **3** *and HF-treated EPS B40.*—In Fig. 4(c) and (d), the 1D ^{1}H NMR spectra of the undecamer (c) and HF-treated EPS B40 (d) are shown. The fact that a homologous series of oligomers was released makes it reasonable to extrapolate the results from **1** and **2** to the undecamer and the polymer. Comparison of the spectra from the heptamer (Fig. 4(b)), the undecamer (Fig. 4(c)) and the polymer (Fig. 4(d)) shows a gradual decrease in intensity of the resonances from the anomeric protons of sugar residues **A**, **B**, $\mathbf{C}^{\alpha/\beta}$ and **D** with increasing degree of polymerisation. In the undecamer, a new anomeric resonance was present (δ 4.69, having partial overlap with **A** H-1) arising from the 1,4-linked residue **D**. If we extrapolate the results from the oligomers to the polymer, the latter consists of sugar residues **D**–**G**, confirming the proposed structure. In the spectrum of the polymer, low intensities of unsubstituted galactosyl residues (**B**) can be seen, which agrees with the partial removal of rhamnosyl substituents upon HF modification.

The NMR results of (the oligomers of) HF-treated EPS B40 together with the analysis of the absolute configuration prove the strong suggestion [10,24] that EPS B40 has the same chemical structure as EPS SBT 0495 [25]. However, in HF-modified EPS our assignment of the proton signals of the β-D-glucopyranosyl residues was different from the assignment reported by Nakajima et al. [25], whereas the anomeric ^{13}C assignments were similar. Based on our assignment of the protons of the trimer and the heptamer, we cannot conclude other than that the proton chemical shifts of residue **F** (H-1 δ 4.52, etc.) belong to the glucosyl residue designated as Glc *B* by Nakajima et al. [25] (H-1 δ 4.653, etc.). Furthermore, the proton chemical shifts of (1→4)-linked glucosyl residue **D** (H-1 δ 4.69 in the undecamer) belong to the glucosyl residue designated as Glc *A* by Nakajima et al. [25] (H-1 δ 4.501, etc.).

4. Discussion

The results of the NMR analyses of the trimer **1** and the heptamer **2** demonstrated that endoV was able to cleave the β-(1→4) linkage between two glucosyl residues, resulting in oligomers containing an unsubstituted galactosyl residue adjacent to the glucose at the reducing side of the linkage cleaved. Based on the specific series of oligomers released by endoV and on the NMR results of **1** and **2**, the mode of action of endoV towards HF-treated EPS B40 can be summarised as is shown in Fig. 6. It should be realised that the relative amount of unsubstituted galactosyl residues drawn in this figure is too high; it was measured to be ca. 20% [10]. Therefore, the possibility for the liberation of larger oligomers (Figs. 1 and 2) is not depicted in Fig. 6. Nevertheless, Fig. 6 clearly shows that endoV is not able to release oligomers with a rhamnosyl-containing 'repeating unit' at the reducing end, which is important information about the mode of action of endoV towards this substrate.

Høj et al. [2] suggested that the substrate specificity of glycosyl hydrolases is determined by their ability to bind different polysaccharides in their substrate-binding sites and by the position of the glycosidic linkage in rela-

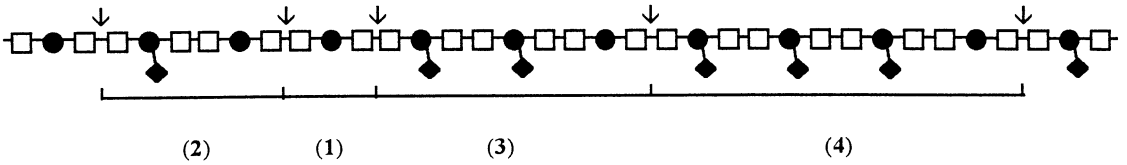

Fig. 6. Mode of action of endoV towards HF-treated EPS B40. In order to show the diversity of oligomers, the relative amount of rhamnosyl substitution drawn in the figure is lower than has been measured in the HF-treated polymer. □, β-D-Glc*p*-(1→4); ●, β-D-Gal*p*-(1→4); ◆, α-L-Rha*p*-(1→2). Sites of endoV attack are indicated by arrows. The resulting oligomers in this example are: trimer **1**, heptamer **2**, undecamer **3**, and pentadecamer **4**.

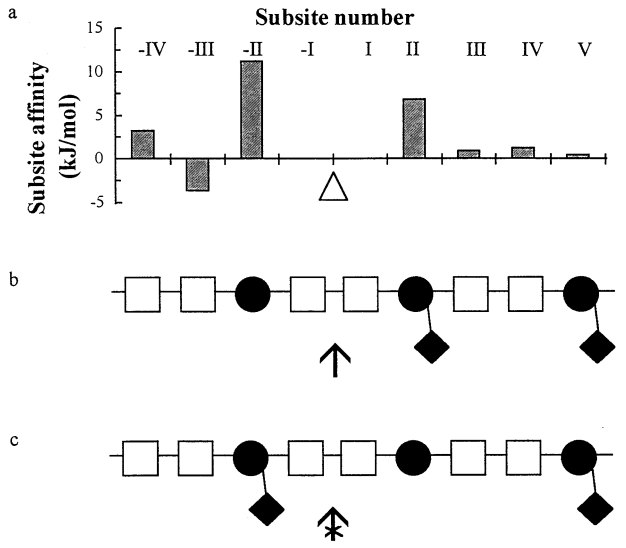

Fig. 7. Subsite interaction of endoV with HF-treated EPS B40. (a) Simplified histogram of subsite interaction energy with Glc residues of cellodextrins for endoV of *T. viride* as described by Vincken et al. [12]. (b) HF-treated EPS B40 fitted in the subsite of endoV in a way that cleavage will occur. (c) HF-treated EPS B40 fitted in the subsite of endoV in a way that cleavage will not occur. △, catalytic group; □, β-D-Glc*p*-(1→4); ●, β-D-Gal*p*-(1→4); ◆, α-L-Rha*p*-(1→2). Sites of endoV attack are indicated by arrows.

tion to the catalytic amino acids. Thus, the first step in enzymic hydrolysis of polysaccharides can be envisaged as binding of several glycosyl residues with an array of subsites. The subsite structure of endoV from *T. viride* (Fig. 7(a)) has been elucidated according to the method of Suganuma et al. [26] using homologous cellodextrins [12]. Subsite affinity is defined as the decrease in free energy upon interaction of an enzyme subsite with a glycosyl residue. Each subsite interacts with one sugar residue. By fitting HF-treated EPS B40 along the subsites in a way that endoV is able to cleave between the adjacent (1→4)-linked glucosyl residues (Fig. 7(a) and (b)), it is remarkable that the subsites with the highest affinity (−II and II), at least for glucosyl residues, interact with galactosyl residues. Since D-glucose and D-galactose are C-4 epimers, it can be concluded that subsites −II and II are tolerant of the different configurations of the hydroxyl group at C-4. The ability of other glucanases to accept epimeric monosaccharides in their binding sites has previously been recognised for *Rhizopus arrhizus* (1→3)-β-glucan endohydrolase (EC 3.2.1.6), which also recognises galactose [27] and mannose [28]. The binding of HF-treated EPS B40 with the subsites of endoV is not hindered by the presence of a rhamnosyl residue linked to the galactosyl residue at subsites II and V, since endoV is still able to cleave (Fig. 7(a) and (b)). As described above, endoV is not able to release oligomers with a rhamnosyl substitution in the 'repeating unit' at the reducing end. In Fig. 7(c), HF-treated EPS B40 is fitted along the subsites in a way that endoV is not able to cleave between the glucosyl residues. It is clear that endoV is hindered by the presence of a rhamnosyl residue linked to the galactosyl residue at subsite −II.

The mode of action of endoV towards potato xyloglucan as described by Vincken et al. [5] indicates that endoV is not hindered by the presence of a xylosyl residue linked to a glucosyl residue at subsite −II. This suggests that the activity of endoV is influenced by the type of sugar of the substituent and/or the type of linkage involved in the substitution of the residue at subsite −II, rather than substitution itself.

The release of oligomer **1** (trimer) (Fig. 3) is very interesting for the mode of action of endoV, especially since the pattern of release is similar to that of oligomer **2** (not shown). EndoV is able to release **1** if at least two adjacent repeating units do not contain rhamnosyl substituents (Fig. 6). This means that subsite II is filled with a galactosyl residue without rhamnosyl substitution, for at least one of the two sites of attack necessary to release oligomer **1**. For the release of oligomers **2**, **3**, **4**, etc., subsite II is always filled with a galactosyl residue substituted with a rhamnosyl residue. Since the release of oligomer **1** at the beginning of the incubation is similar to the release of **2**, it can be concluded that endoV does not prefer unsubstituted galactosyl residues at subsite II above galactosyl residues substituted with a rhamnosyl residue.

The specificity of EndoV from *T. viride* has been shown to be broader than that of the true cellulases since it is able to degrade xylan [3], xyloglucan and possibly mannan [5]. Present study shows that endoV is also able to degrade HF-modified EPS B40. Table 3 sum-

Table 3
Summary of the different modifications of EPS B40 and the release of phosphate and oligosaccharides from the resulting polymers after incubation with Maxazyme Cl or purified endoV (P, Phosphate; □, β-D-Glc*p*-(1→4); ●, β-D-Gal*p*-(1→4) or α-D-Gal*p*-(1→P); ◆, α-L-Rha*p*-(1→2); the approximate relative amount of the remaining rhamnosyl residues (100% = 1.0) is given in case rhamnose had been partially removed. –, no release; +, release; ++, high release of small oligomers)

EPS B40 modification	Structure of 'repeating unit'	Maxazyme Cl		Purified endoV
		P-release by phosphatase	Oligosaccharide(s) release	Oligosaccharide(s) release
Native EPS	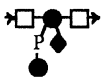	–	–	n.d.[a]
H_2SO_4-treated		–	–	n.d.
CF_3CO_2H-treated	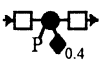	+	+[b]	–
HF-treated	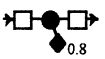	n.r.[c]	+	+
HF *and* CF_3CO_2H-treated	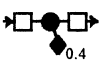	n.r.	++	++

[a] not determined since the crude enzyme preparation was negative.
[b] only the trimer was released.
[c] not relevant since phosphate was not present in the substrate.

marises the different modifications of EPS B40 and the enzyme activity of Maxazyme Cl and purified endoV on the resulting polymers. Chemical modification with HF was performed because native EPS B40 appeared to be resistant to degradation by all enzyme preparations examined and we thought that this was caused by the phosphate substituent. The removal of phosphate with HF simultaneously released ca. 20% of the rhamnosyl substitutions and this appeared to be critical for the activity of endoV. Later we found that removal of rhamnosyl and galactosyl substituents by mild CF_3CO_2H treatment made the substrate accessible to a phosphatase. In retrospect, mild CF_3CO_2H hydrolysis can be used as an alternative to HF treatment to modify EPS B40 since it liberates terminally linked galactose and (at least part of) rhamnose. The resulting polymer can be dephosphorylated by a phosphatase present in Maxazyme CL and subsequently degraded by endoV in Maxazyme CL.

The present study shows that (enzymic) modifications of EPS are not only helpful for the structural characterisation of EPS, but that they can also be useful to unravel the mode of action of the enzymes used.

Acknowledgements

We thank R.A.M. van der Hoeven for the HPAEC/MS measurements and J.-P. Vincken for fruitful discussions. This work was financially supported by the Ministry of Economic Affairs, the Ministry of Education, Culture and Science and the Ministry of Agriculture, Nature Management and Fishery in the framework of an industrial relevant research programme of the Netherlands Association of Biotechnology Centres in The Netherlands (ABON).

References

[1] M.A. Anderson, B.A. Stone, *FEBS Lett.*, 52 (1975) 202–207.
[2] P.B. Høj, E.B. Rodriguez, R.V. Stick, B.A. Stone, *J. Biol. Chem.*, 264 (1989) 4939–4947.
[3] G. Beldman, A.G.J. Voragen, F.M. Rombouts, M.F. Searle-van Leeuwen, W. Pilnik, *Biotechnol. Bioeng.*, 31 (1988) 160–167.
[4] P. Biely, M. Vršanská, M. Claeyssens, *Eur. J. Biochem.*, 200 (1991) 157–163.
[5] J.-P. Vincken, A.J.M. Wijsman, G. Beldman, W.M.A. Niessen, A.G.J. Voragen, *Carbohydr. Res.*, 288 (1996) 219–232.
[6] R. Macarrón, C. Acebal, M.P. Castillón, M. Claeyssens, *Biotechnol. Lett.*, 18 (1996) 599–602.
[7] P. Cescutti, R. Toffanin, W.F. Fett, S.F. Osman, P. Pollesello, S. Paoletti, *Eur. J. Biochem.*, 251 (1998) 971–979.
[8] G. Beldman, M.F. Searle-van Leeuwen, F.M. Rombouts, A.G.J. Voragen, *Eur. J. Biochem.*, 146 (1985) 301–308.
[9] I.W. Sutherland, *Biotechnology of Microbial Exopolysaccharides*, Cambridge University Press, Cambridge, 1990, pp. 12–54.
[10] W.H.M. van Casteren, C. Dijkema, H.A. Schols, G. Beldman, A.G.J. Voragen, *Carbohydr. Polym.*, 37 (1998) 123–130.
[11] R. Tuinier, P. Zoon, C. Olieman, M.A. Cohen Stuart, G.J. Fleer, C.G. de Kruif, *Biopolymers*, 49 (1999) 1–9.
[12] J.-P. Vincken, G. Beldman, A.G.J. Voragen, *Carbohydr. Res.*, 298 (1997) 299–310.
[13] M.M. Bradford, *Anal. Biochem.*, 72 (1976) 248–254.
[14] P.S. Chen Jr., T.Y. Toribara, H. Warner, *Anal. Chem.*, 28 (1956) 1756–1758.
[15] G.J. Gerwig, J.P. Kamerling, J.F.G. Vliegenthart, *Carbohydr. Res.*, 62 (1978) 349–357.
[16] C.T.M. Fransen, K.M.J. van Laere, A.A.C. van Wijk, L.P. Brüll, M. Dignum, J.E. Thomas-Oates, J. Haverkamp, H.A. Schols, A.G.J. Voragen, J.P. Kamerling, J.F.G. Vliegenthart, *Carbohydr. Res.*, 314 (1998) 101–114.
[17] D. Marion, K. Wüthrich, *Biochem. Biophys. Res. Commun.*, 113 (1983) 967–974.
[18] A. Bax, S.W. Sparks, D.A. Torchia, *J. Am. Chem. Soc.*, 110 (1988) 7926–7927.
[19] R.A.M. van der Hoeven, U.R. Tjaden, J. van der Greef, W.H.M. van Casteren, H.A. Schols, A.G.J. Voragen, C. Bruggink, *J. Mass Spectrom.*, 33 (1998) 377–386.
[20] I. Hancock, I. Poxton, *Bacterial Cell Surface Techniques*, Wiley, Chichester, 1988, p. 179.
[21] J. Lemoine, F. Chirat, J.-M. Wieruszeski, G. Strecker, N. Favre, J.-R. Neeser, *Appl. Environ. Microbiol.*, 63 (1997) 3512–3518.
[22] K. Bock, H. Thøgersen, *Annu. Rep. NMR Spectrosc.*, 13 (1982) 1–57.
[23] P.-E. Jansson, J. Lindberg, K.M.S. Wimalasiri, M.A. Dankert, *Carbohydr. Res.*, 245 (1993) 303–310.
[24] R. van Kranenburg, J.D. Marugg, I.I. van Swam, N.J. Willem, W.M. de Vos, *Mol. Microbiol.*, 24 (1997) 387–397.
[25] H. Nakajima, T. Hirota, T. Toba, T. Itoh, S. Adachi, *Carbohydr. Res.*, 224 (1992) 245–253.
[26] T. Suganuma, R. Matsuno, M. Ohnishi, K. Hiromi, *J. Biochem.*, 84 (1978) 293–316.
[27] M.A. Anderson, B.A. Stone, *Carbohydr. Res.*, 61 (1978) 479–492.
[28] L. Cardemil, C.P. Wolk, *J. Biol. Chem.*, 254 (1979) 736–741.